Inorganic Chemistry

Open Access
This article is licensed under CC-BY 4.0

pubs.acs.org/IC
Article

Near Infrared−Circularly Polarized Luminescence/Circular Dichroism Active Yb(III) Complexes Bearing Both Central and Axial Chirality

Silvia Ruggieri,* Oliver George Willis, Silvia Mizzoni, Enrico Cavalli, Martina Sanadar, Andrea Melchior, Francesco Zinna, Lorenzo Di Bari, Giorgiana Denisa Bisag, Mariafrancesca Fochi, Luca Bernardi, and Fabio Piccinelli*

Cite This: *Inorg. Chem.* 2025, 64, 5505−5512

Read Online

ACCESS | Metrics & More | Article Recommendations | Supporting Information

ABSTRACT: In this contribution, we present new NIR-CPL/CD active Yb(III) complexes, which are synthesized by combining two ligands characterized by different types of chirality: central and axial chirality. The ligand bearing central chirality is represented by the neutral *trans-N,N′*-bis(2-pyridylmethylidene)-1,2-(*R,R* or *S,S*) cyclohexanediamine (**L**), whereas the axial ligand is 1,1′-binaphthyl-2,2′-diol (BINOL-H_2). A combined ^{1}H NMR, thermodynamic (spectrophotometric titrations), and theoretical (DFT structural calculations) study is presented, revealing the high stability in the methanol solution of the homochiral C_2-symmetric anionic $[Yb\mathbf{L}(BINOL)_2]^-$ complexes, in which the two labile BINOLate molecules exhibit the same stereochemistry (*R* or *S*). The metal ion-related optical and chiroptical properties of the complexes in the near-infrared spectral region are here presented and discussed: while the axial chirality dominates the circularly polarized luminescence features, the NIR-CD signal is affected by both chiral elements.

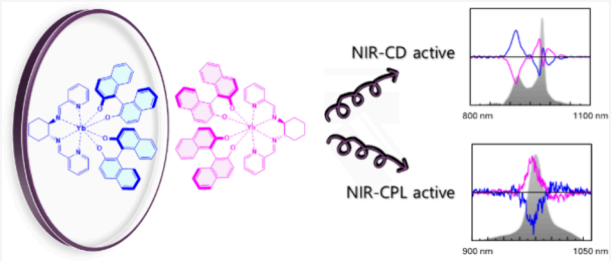

INTRODUCTION

It is well-known that the 650−1400 nm range, called the biological window, is a very attractive region for biological imaging.[1−7] The emission of near-infrared (NIR) emitting Ln(III) complexes[8−13] falls in this spectral region where common biological tissues are transparent and the radiations cause reduced damage due to photobleaching.[14] Circularly polarized luminescence (CPL) in this region should benefit from the specificity, selectivity, and sensitivity, which are related to the chiroptical counterpart of emission spectroscopy.[3,15−17]

Moreover, NIR-CPL[18,19] could expand the potential applications of these complexes to the technological field, making Ln(III) species good candidates also for optoelectronic devices,[20,21] OLED,[22,23] or laser systems.[24]

An efficient NIR-CPL activity is expected in the case of chiral Yb(III)-based complexes in which the spin allowed $^2F_{5/2} \rightarrow {}^2F_{7/2}$ emission transition, around 980 nm, is characterized by a high value of the rotational strength and sizable value of the emission dissymmetry factor g_{Em}.[25] In addition, in order to increase the emission intensity of Ln(III) ions, suitable organic sensitizers are usually linked to the metal center, triggering the well-known nonradiative ligand-to-metal energy transfer processes (*antenna* effect).[26−28]

One common drawback affecting the luminescence emission efficiency of NIR emitting Ln(III) complexes is represented by multiphonon relaxation (MPR) processes involving the stretching vibrations of the X-H bonds (X = C, N, O) present in the coordinating ligands and solvent molecules.[29] Therefore, in an aqueous solution, water molecules in the proximity of the metal ion can significantly reduce the $^2F_{5/2}$ excited state lifetime of Yb(III) and also its luminescence efficiency. The exclusion of water from the inner coordination sphere is strongly recommended to ensure a sufficient luminescence efficiency of the emitting metal ion. This has been achieved in cases such as a bicapped Yb(III) ion, utilizing a porphyrin-based double-decker[30] or with hydrophobic complexes.[31] Moreover, the detrimental effect of MPR can be significantly limited by embedding luminescent complexes in polymeric nanoparticles. Previous studies have demonstrated that poly lactic-*co*-glycolic acid (PLGA) is an attractive candidate for encapsulating and thus protecting Yb(III) complexes.[32] Several years ago, Arrico et al. proposed to quantify the overall efficiency of circularly polarized emitters by means of the circularly polarized luminescence brightness (B_{CPL}) factor. This efficiency is dependent not only on the degree of the CP emission's dissymmetry (the relative amount of emitted left- compared to right-handed photons) but also on the molar extinction coefficient and the quantum yield of the

Received: December 19, 2024
Revised: February 7, 2025
Accepted: March 4, 2025
Published: March 13, 2025

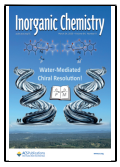

Downloaded via UNIV DEGLI STUDI DI VERONA on May 14, 2025 at 16:22:51 (UTC).
See https://pubs.acs.org/sharingguidelines for options on how to legitimately share published articles.

ACS Publications
© 2025 The Authors. Published by American Chemical Society

https://doi.org/10.1021/acs.inorgchem.4c05420
Inorg. Chem. 2025, 64, 5505−5512

compound.[33] In other words, during the design of an efficient CPL emitter based on Ln(III) complexes, strong absorption of the chromophore, an efficient *antenna* effect, and negligible nonradiative phenomena like MPR must be considered. As for the ligands conferring CPL activity to Yb(III) ion, we focus our attention on two kinds of organic molecules: the neutral *trans*-*N*,*N*′-bis(2-pyridylmethylidene)-1,2-(*R*,*R* or *S*,*S*) cyclohexanediamine (**L**) bearing two stereocenters and the well-known 1,1′-binaphthyl-2,2′-diol (BINOL-H_2)[34−37] exhibiting axial chirality (Figure 1).

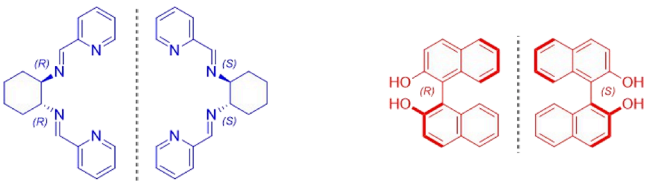

Figure 1. Central chiral ligand **L** (left) and axial chiral ligand BINOL-H_2 (right).

Yb(III) ion displays a g_{lum} factor $(2(I_L - I_R)/(I_L + I_R))$ of |0.03| and |0.17| when the first or the second ligand is employed in [Yb**L**(tta)$_2$]CH_3COO; tta = 2-thenoyltrifluoroacetonate[32] and [(Binol)$_3$YbNa$_3$], respectively.[38]

The idea at the basis of the present study is to combine the two different kinds of stereogenic elements (central and axial chirality) to modulate the lanthanide-centered chiroptical features (NIR-CD and CPL, in particular).

To the best of our knowledge, this combination is performed for the first time in the literature in the case of Yb(III) complexes.

In detail, by binding these two ligands (one equivalent of **L** and two equivalents of the deprotonated form BINOL^{2-}) to the Yb(III) ion, several stereochemical combinations are in principle possible, all producing negatively charged complexes. In particular, focusing attention on BINOL stereochemistry, two diastereoisomeric homochiral species (i.e., [Yb(*R*,*R*)-**L**(*S*-BINOL)$_2$]$^-$ and [Yb(*R*,*R*)-**L**(*R*-BINOL)$_2$]$^-$ and their enantiomers) and one heterochiral enantiomers pair (i.e., [Yb(*R*,*R*)-**L**(*S*-BINOL)(*R*-BINOL)]$^-$ and [Yb(*S*,*S*)-**L**(*R*-BINOL)(*S*-BINOL)]$^-$ could be obtained. In this contribution, we demonstrate the higher stability of the homochiral species compared with the heterochiral species (Figure 2).

The stability of these complexes in methanol solution was determined as well as their DFT minimum energy structure. A detailed optical and chiroptical characterization in the NIR spectral region at around 1000 nm is presented.

■ EXPERIMENTAL SECTION

Solvents were purchased from Fisher Scientific, VWR Chemicals, or Carlo Erba Reagents and used without further purification. Starting materials were purchased from Sigma-Aldrich and Alfa Aesar. Yb$(NO_3)_3$·5H_2O (Aldrich, 98%) has been stored under vacuum for several days at 80 °C and then transferred into a glovebox.

Elemental Analysis. Total carbon, hydrogen, nitrogen, and sulfur concentrations were determined by flash combustion using an elemental analyzer (CHNS vario Macro Cube, Elementar, Germany). Sulfanilamide (Elementar Analysensysteme GmbH, Germany) was used as a standard. The QA/QC was generally >96% for all elements.

Infrared Absorption. IR spectra were collected by means of a PerkinElmer FT-IR spectrum two spectrophotometer (resolution of 4 cm^{-1}).

ESI-MS. Electrospray ionization mass spectra (ESI-MS) were recorded in methanol solutions on a Waters Micromass ZQ 4000 instrument operating in positive ion mode. Experimental conditions: 3.53 kV ES-probe voltage, 20 V cone potential, 200 L h^{-1} flow of N_2 spray-gas, and incoming-solution flow of 20 μL min^{-1}.

NMR. ^{1}H NMR spectra were recorded on a Varian Mercury 400 or Inova 600 spectrometer. Chemical shifts (d) are reported in parts per

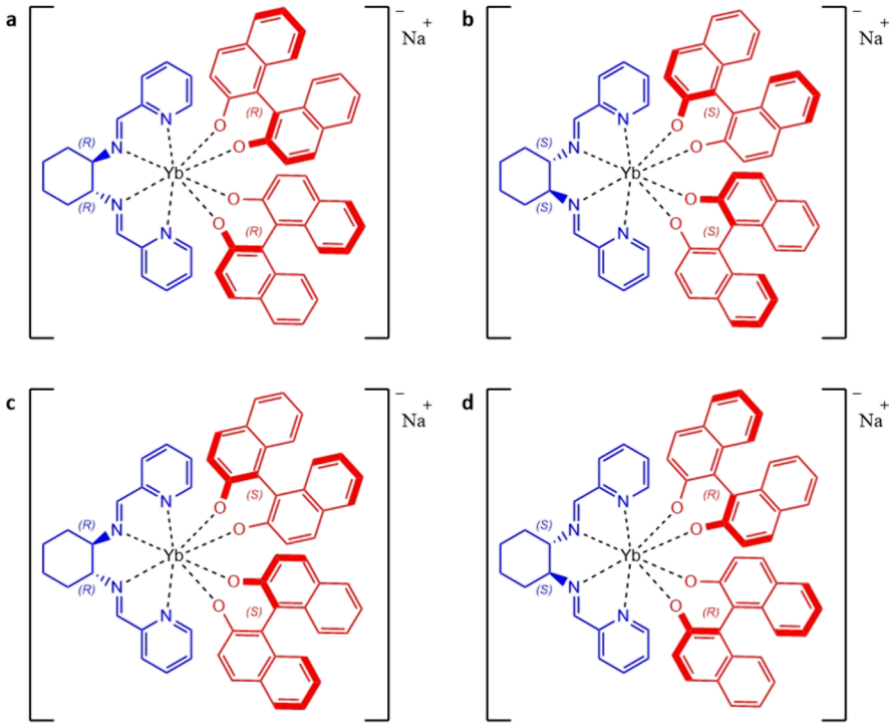

Figure 2. Complexes investigated in this work: (a) [Yb(*R*,*R*)-**L**(*R*-BINOL)$_2$]Na, (b) [Yb(*S*,*S*)-**L**(*S*-BINOL)$_2$]Na, (c) [Yb(*R*,*R*)-**L**(*S*-BINOL)$_2$]Na, and (d) [Yb(*S*,*S*)-**L**(*R*-BINOL)$_2$]Na.

https://doi.org/10.1021/acs.inorgchem.4c05420
Inorg. Chem. 2025, 64, 5505−5512

million relative to TMS. Coupling constants (J) are reported in Hertz (Hz). Splitting patterns are designated as s (singlet), d (doublet), t (triplet), q (quartet), and m (multiplet).

Total Luminescence (TL). The emission and decay time measurements were carried out by means of an Edinburgh FLS1000 spectrofluorometer equipped with both continuous and pulsed Xe lamps, a double excitation monochromator, a single emission monochromator, and a N_2-cooled NIR extended photomultiplier for the detection of the emitted signal. All the spectra were measured at room temperature and corrected for the spectral responsiveness of the setup.

NIR-CPL Measurements. NIR-CPL spectra were recorded using the home-built spectrofluoropolarimeter, equipped with a Hamamatsu, R316 Ag−O−Cs photomultiplier tube, as described in ref 20. The spectra were collected under 365 nm irradiation from a commercial LED source, using a 90° geometry between the excitation and detection direction. All the NIR-CPL spectra were recorded on 1 mM CD_3OD solutions in 1 cm semimicro (aperture 4 mm) optical glass cells using the following parameters: scan speed of 0.5 nm/s, integration time of 4 s, photomultiplier tube driving voltage of 1100 V, accumulations of 6−9, and em. bandwidth of >10 nm.

UV−vis/ECD (Electronic Circular Dichroism) and NIR-CD Measurements. UV−vis spectra were recorded using a Jasco-V650 spectrophotometer in the spectral range of 200 to 400 nm. All samples were measured in 1 mM CD_3OD solutions at room temperature in a 0.01 cm optical glass cell. The same solutions and cells were used to record CD spectra using a J1500 spectropolarimeter. NIR-CD measurements were performed by using a Jasco J-1500 spectropolarimeter equipped with an NIR detector (EXIG-542). Complexes were measured in DCM of 10 mM due to improved solubility. All complexes were measured in 1 cm optical glass cells with parameters as follows: scan speed of 100 nm/min, bandwidth of 10 nm, integration time of 4 s, and accumulations of 8.

DFT Calculations. All molecular structures of the complexes were obtained by means of DFT calculations run in Gaussian 16 (version A.03).[39] The ωB97X−D functional[40] was used with the 6-31+G(d) basis set for all ligand atoms and MWB28 pseudopotential and valence electrons basis set for the metal ion.[41] The paramagnetic Yb(III) ion was replaced by a similar Lu(III) ion. As for structural properties and the differences in the total energies, the Lu(III) ion can be considered the best computational model for Yb(III) since it has almost the same ionic radius as Yb(III), but its closed shell electron configuration enables to run less computationally demanding calculations. Geometry optimizations were carried including solvent (methanol) effects by means of the polarizable continuum model (PCM).[42]

Vibrational analysis was performed to confirm that the obtained structures were energy minima.

Synthesis of the Complexes. The *trans-N,N′*-bis(2-pyridylmethylidene)-1,2-(*R,R* or *S,S*) cyclohexanediamine ligand (**L**) was synthesized as reported in the literature.[43]

[Yb(**L**)(BINOL)$_2$]Na isomers (Figure 2) were synthesized as follows. At room temperature, $Yb(NO_3)_3{\cdot}5H_2O$ (80 mg, 0.18 mmol) was added to a clear light brown methanol solution of *trans-N,N′*-bis(2-pyridylmethylidene)-1,2-(*R,R* or *S,S*) cyclohexanediamine (**L**) (52 mg, 0.18 mmol). In another flask, 1,1′-binaphthyl-2,2′-diol (BINOL-H_2) (*S* or *R*) (102 mg, 0.36 mmol) was solubilized in methanol and added to a solution of NaOMe (39 mg, 0.72 mmol) in the same solvent. The deprotonated BINOL ligand was slowly added to the cloudy light brown solution containing the Ln(III) complex. The final yellow and cloudy mixture was stirred for 3 h. Then, the solvent was removed under reduced pressure, and the desired product was obtained as a yellow powder upon extraction in dichloromethane (2 × 7 mL) followed by solvent removal in vacuo. The chemical yield was around 90%, for the isomers mixture, which was obtained with a high degree of purity, as demonstrated by the following characterization analysis.

The Y(III) counterpart of the isomer c (Figure 2) [Y(*R,R*)-**L**(*S*-BINOL)$_2$]Na was synthesized by following the aforementioned protocol but using YCl_3 instead of $Yb(NO_3)_3$. The chemical yield was 85%.

Elemental analysis:calc. for $C_{58}H_{46}N_4NaO_5Yb$ (MW 1075.07 g/mol), corresponding to [Yb(**L**)(BINOL)$_2$]Na·H_2O: C, 64.80; H, 4.31; N, 5.21. Found (isomer a): C, 64.91; H, 4.27; N, 5.24; (isomer b): C, 64.85; H, 4.28; N, 5.26; (isomer c): C, 64.76; H, 4.25; N, 5.25; (isomer d): C, 64.75; H, 4.29; N, 5.26. Calc. for $C_{58}H_{46}N_4NaO_5Y$ (MW 990.92 g/mol), corresponding to [Y(**L**)(BINOL)$_2$]Na·H_2O: C, 70.30; H, 4.68; N, 5.65. Found: C, 70.52; H, 4.81; N, 5.58.

In the infrared-absorption spectrum of [Yb(*S,S*)-**L**(*R*-BINOL)$_2$]Na (chosen as representative) (Figure S1) the signals related to OH stretching of *R*-BINOL-H_2 at ν_{OH} = 3500 and 3420 cm^{-1} disappear. The signal related to the C═N stretching ($\nu_{C=N}$ = 1650 cm^{-1}) is present corroborating the presence of the imine functional group of the **L** ligand in the complex.

ESI-MS (scan ES+, m/z) [Yb**L**(BINOL)$_2$][Na]: 1058 {[Yb**L**(BINOL)$_2$][H][Na]}$^+$, 1036 {[Yb**L**(BINOL)$_2$][H]$_2$}$^+$, 782 {[Yb(BINOL)$_2$][H][K]}$^+$, 750 {Yb**L**(BINOL)}$^+$ for all the isomers (see Figure S2 and Table S1). [Y**L**(BINOL)$_2$][Na]: 973 {[Y**L**(BINOL)$_2$][H][Na]}$^+$, 951 {[Y**L**(BINOL)$_2$][H]$_2$}$^+$, 697 {Y**L**(BINOL)CH_3OH}$^+$, 665 {Yb**L**(BINOL)}$^+$ (Figure S3 and Table S2).

■ RESULTS AND DISCUSSION

Density Functional Theory (DFT) Calculation and ^{1}H NMR Investigation. In the absence of single crystals of good quality for the crystal structure determination by means of X-ray diffraction, density functional theory (DFT) calculations were performed on three representative species, whose minimum energy structures are reported in Figure 3.

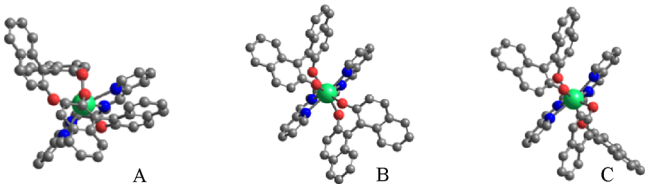

Figure 3. Minimum energy structures of (A) [Lu(*R,R*)-**L**(*R*-BINOL)$_2$]$^-$, (B) [Lu(*R,R*)-**L**(*S*-BINOL)$_2$]$^-$, and (C) [Lu(*R,R*)-**L**(*R*-BINOL)(*S*-BINOL)]$^-$. Additional images with different orientations can be found in Figure S7.

In all cases, the metal ion (Lu was used to model Yb) displays an 8-fold coordination characterized by the four nitrogen atoms of the DACH-based **L** ligand and four oxygen atoms (two atoms for each BINOL molecule). The two BINOL ligands are bound above and below the plane defined by the **L** ligand.

Regarding the configuration of the binaphthol units, the calculated difference in energy between the homochiral [Lu(*R,R*)-**L**(*R*-BINOL)$_2$]$^-$ (A) and [Lu(*R,R*)-**L**(*S*-BINOL)$_2$]$^-$ (B) species (Figure 3) is $\Delta E = E(B) - E(A) = 1.3$ kcal mol^{-1} suggesting similar stability of the two isomers. On the contrary, the heterochiral [Lu(*R,R*)-**L**(*R*-BINOL)(*S*-BINOL)]$^-$ species (C) is significantly less stable [$\Delta E = E(C) - E(A) = 3.2$ kcal mol^{-1}] and its presence in a complex solution containing Yb^{3+}, (*R,R*)-**L**, (*R*-BINOL), and (*S*-BINOL) can be in principle neglected.

In order to gain more insight into the structure of the Yb(III) complexes in solution, we performed a ^{1}H NMR analysis. Since the resulting spectra were characterized by very broad peaks and therefore they were not informative, we investigated the ^{1}H NMR spectra of the representative Y(III) complexes, i.e., [Y(*R,R*)-**L**(*S*-BINOL)$_2$]Na. The diamagnetic

https://doi.org/10.1021/acs.inorgchem.4c05420
Inorg. Chem. 2025, 64, 5505−5512

properties of Y(III) will help to obtain more information about the nature and the structure of the complex, considering the very small difference of the ionic radii of Yb(III) and Y(III) (0.03 Å for 8-fold coordination), which makes the Y(III) a suitable structural equivalent of Yb(III). The [Y(*R*,*R*)-**L**(*S*-BINOL)$_2$]Na complex was analyzed using ^{1}H NMR (Figure S4) and gCOSY ^{1}H-{^{1}H} (CD_2Cl_2 solution) (Figure S5). As detailed in the Supporting Information (Section 1.3), while the pyridinic, iminic, and methinic protons are readily identifiable in the spectrum and suggest a C_2 symmetry of the molecule, some signals related to aromatic protons of the BINOLate ligands are very broad, and only five aromatic protons (H_{Ar}) are clearly identified in the spectrum (Figure S4). The broadening of these signals should be strongly connected with the lability of metal-BINOL bonds in solution as previously observed for the Yb(III) ion.[44,45] In order to resolve the broad aromatic peaks of BINOLate, variable temperature (VT) ^{1}H NMR experiments in CD_3CN have been carried out in the range from −30 to 65 °C as shown in Figure S6. Despite this attempt, only a partial resolution of the two broad aromatic bands has been obtained upon heating the sample, so the integration of these signals cannot be used to confirm the stoichiometry of the complex, which has been determined by means of other experimental techniques (elemental analysis and ESI-MS).

Thermodynamic Study. To experimentally determine the stability of the homochiral complexes, spectrophotometric titrations in the methanol solution of both BINOL enantiomers with [Yb(*R*,*R*)-**L**]$(NO_3)_3$ (Yb(*R*,*R*)-**L** in Table 1) were carried out (Figure S9). As suggested by DFT calculations, the two homochiral complexes, [Yb(*R*,*R*)-**L**(*R*-BINOL)$_2$]$^-$ and [Yb(*R*,*R*)-**L**(*S*-BINOL)$_2$]$^-$, show a very similar stability (Table 1).

Table 1. Formation Constants (logβ) in Dry Methanol for the Yb(III) Complexes under Investigation

equilibria	logβ
Yb(*R*,*R*)-**L** + *S*-BINOL ⇌ Yb(*R*,*R*)-**L**(*S*-BINOL)	7.57 (±0.07)
Yb(*R*,*R*)-**L** + 2*S*-BINOL ⇌ Yb(*R*,*R*)-**L**(*S*-BINOL)$_2$	13.3 (±0.1)
Yb(*R*,*R*)-**L** + *R*-BINOL ⇌ Yb(*R*,*R*)-**L**(*R*-BINOL)	7.87 (±0.04)
Yb(*R*,*R*)-**L** + 2*R*-BINOL ⇌ Yb(*R*,*R*)-**L**(*R*-BINOL)$_2$	13.2 (±0.1)

Total Luminescence (TL) and Luminescence Decay Kinetics. From the inspection of the absorption spectra of the complexes (Figure S10), the band just below 300 nm (ε_{max} = 27000 $M^{-1}cm^{-1}$) may be attributed to transitions of both BINOL^{-2} and pyridine ring of **L** (the $\pi \rightarrow \pi^*$ transition),[32] whereas the more red-shifted band close to 350 nm (ε_{max} = 12000 $M^{-1}cm^{-1}$), to one of the $\pi \rightarrow \pi^*$ of the BINOL^{-2}.[44] Furthermore, the luminescence excitation and emission spectra of methanol solutions (200 μM) of the complexes are shown in Figure 4a.

The excitation profiles demonstrate the presence of an efficient *antenna* effect of both ligands, in particular for BINOL. In fact, the intensity of the peak located around 350 nm is almost twice that of the peak at 300 nm.

The typical luminescence emission spectra of Yb(III) are obtained,[32] dominated by a sharp transition peaking at 980 nm and a more complex manifold in the 900−1100 nm region, associated to the crystal field splitting of the $^2F_{7/2}$ ground state. Upon excitation in the BINOL absorption band (355 nm), the recorded luminescence decay of the $^2F_{5/2}$ excited state of Yb(III) (monitored at 980 nm) in the two samples is similar and follows an exponential decay (Figure 4b). The related lifetimes are 2.49(4) and 2.06(3) μs for [Yb(*R*,*R*)-**L**(*R*-BINOL)$_2$]Na and [Yb(*R*,*R*)-**L**(*S*-BINOL)$_2$]Na, respectively.

As reported in the literature,[46−48] the values of these decay times are compatible with the presence of solvent molecules (i.e., polar protic solvents) in the proximity of Yb(III) capable of quenching its excited state *via* MPR.[49,50] In particular, as the OH group of methanol has high-energy vibrations (3300−3400 cm^{-1}), it can efficiently quench the Ln(III) emitting level.[51]

The slightly shorter lifetime of the [Yb(*R*,*R*)-**L**(*S*-BINOL)$_2$]Na complex can be rationalized by the shorter distance between the solvent molecules and the metal center, found by DFT calculations on the related Lu(III) complexes in the presence of solvent molecules (Figure S8, water was used as a model for methanol). In detail, while in [Lu(*R*,*R*)-**L**(*R*-BINOL)$_2$]Na one solvent molecule lies in the outer coordination sphere, in [Lu(*R*,*R*)-**L**(*S*-BINOL)$_2$]Na, the solvent molecule is closer to the inner coordination sphere, as the solvent is bound, through hydrogen bond, to one oxygen atom of BINOL. In this context, the closer the solvent molecule is to the metal ion, the more efficient the MPR process is and therefore shorter the Yb(III) lifetime.

Chiroptical Spectroscopy. The NIR-CPL spectra of chiral complexes [Yb(*R*,*R*)-**L**(*S*-BINOL)$_2$]Na and [Yb(*R*,*R*)-**L**(*R*-BINOL)$_2$]Na (and the related enantiomers) are reported in Figure 5.

From the inspection of these spectra, we can conclude that the CPL activity of Yb(III) is mainly controlled by the BINOL stereochemistry. In fact, a negative band with a g_{lum} of 0.01 around 980 nm is detected when two *S*-BINOLs are bound to the metal center, regardless of the stereochemistry of the **L** ligand (please refer to the spectra of [Yb(*R*,*R*)-**L**(*S*-BINOL)$_2$]Na and [Yb(*S*,*S*)-**L**(*S*-BINOL)$_2$]Na in Figure 5). To corroborate the dominant role of the BINOL stereochemistry on the NIR-CPL activity of the Yb(III) ion, we performed CPL titration experiments in which the Yb(III) complexes were titrated with the BINOL enantiomer of opposite chirality with respect to the one present in the complex (i.e., [Yb(*R*,*R*)-**L**(*S*-BINOL)$_2$]Na titrated with *R*-BINOL and [Yb(*R*,*R*)-**L**(*R*-BINOL)$_2$]Na titrated with *S*-BINOL). In agreement with the lability of Yb-BINOL bonds in a solution of polar solvents previously discussed,[44,45] a change in the CPL spectrum was observed (Figure 6). In both the titrations, the weak negative CPL band obtained after the addition of 2 equiv of BINOL is consistent with a slightly higher thermodynamic stability of [Yb(*R*,*R*)-**L**(*S*-BINOL)$_2$]Na with respect to [Yb(*R*,*R*)-**L**(*R*-BINOL)$_2$]Na (Table 1).

Contrary to the NIR-CPL activity, the NIR-CD and ECD in the UV region are significantly affected by both kinds of stereogenic elements (Figure 7; see also Figure S10 for ECD spectra).

When keeping the central stereochemistry of the ligand **L** constant, and upon switching the BINOL stereochemistry (passing from [Yb(*R*,*R*)-**L**(*R*-BINOL)$_2$]Na to [Yb(*R*,*R*)-**L**(*S*-BINOL)$_2$]Na), the relative intensity (but not the sign) of the CD peaks changes. On the other hand, the only change of the **L** stereochemistry (i.e., passing from [Yb(*R*,*R*)-**L**(*R*-BINOL)$_2$]Na to [Yb(*S*,*S*)-**L**(*R*-BINOL)$_2$]Na) gives rise to the reversal of the CD peaks signal while also affecting their relative intensities.

https://doi.org/10.1021/acs.inorgchem.4c05420
Inorg. Chem. 2025, 64, 5505−5512

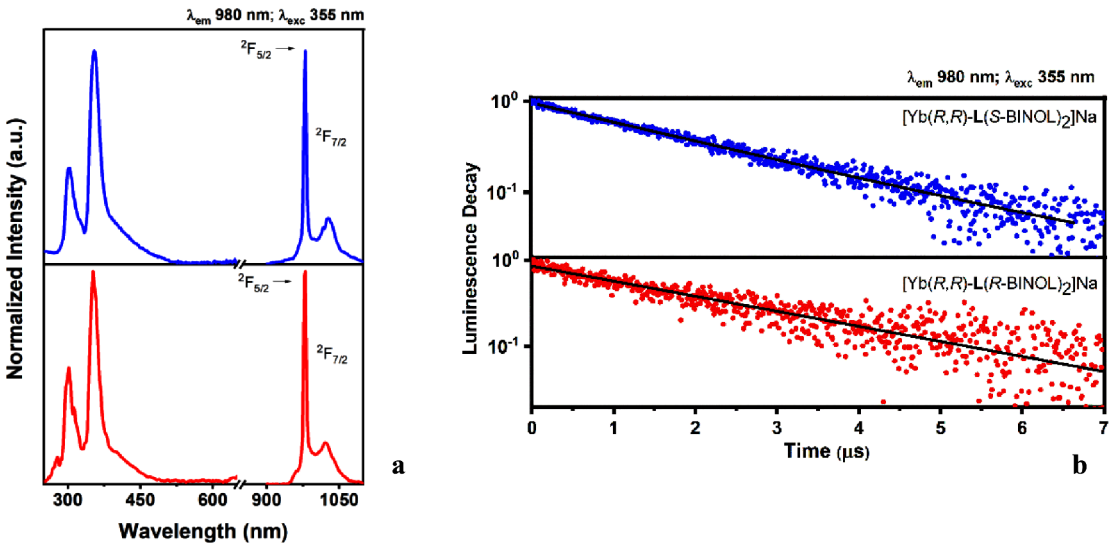

Figure 4. (a) Excitation (left) and emission (right) spectra in methanol solution (200 μM) of the two homochiral complexes [Yb(*R*,*R*)-**L**(*S*-BINOL)$_2$]Na (up) and [Yb(*R*,*R*)-**L**(*R*-BINOL)$_2$]Na (bottom). These spectra are fully superimposable with those of the respective enantiomers [Yb(*S*,*S*)-**L**(*R*-BINOL)$_2$]Na and [Yb(*S*,*S*)-**L**(*S*-BINOL)$_2$]Na; (b) luminescence decay curves of the Yb(III) $^2F_{5/2}$ excited state for methanol solutions (200 μM) of [Yb(*R*,*R*)-**L**(*S*-BINOL)$_2$]Na and [Yb(*R*,*R*)-**L**(*R*-BINOL)$_2$]Na complexes under investigation, chosen as representative. These curves are fully superimposable with those of the respective enantiomers [Yb(*S*,*S*)-**L**(*R*-BINOL)$_2$]Na and [Yb(*S*,*S*)-**L**(*S*-BINOL)$_2$]Na.

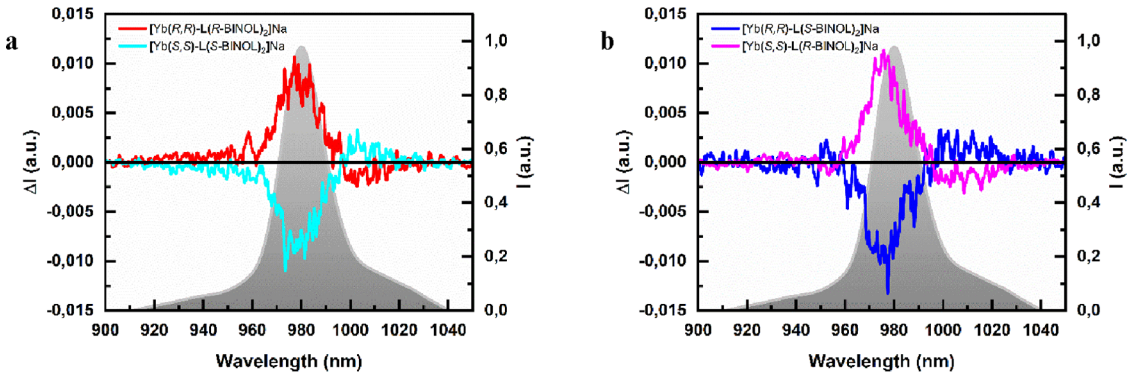

Figure 5. NIR-CPL spectra of 1 mM CD_3OD solutions of the two enantiomeric couples of the investigated Yb(III) complexes. (a) [Yb(*R*,*R*)-**L**(*R*-BINOL)$_2$]Na (red)/[Yb(*S*,*S*)-**L**(*S*-BINOL)$_2$]Na (cyano) and (b) [Yb(*R*,*R*)-**L**(*S*-BINOL)$_2$]Na (blue)/[Yb(*S*,*S*)-**L**(*R*-BINOL)$_2$]Na (magenta). The normalized total emission for each couple is traced in the background. λ_{exc} = 365 nm.

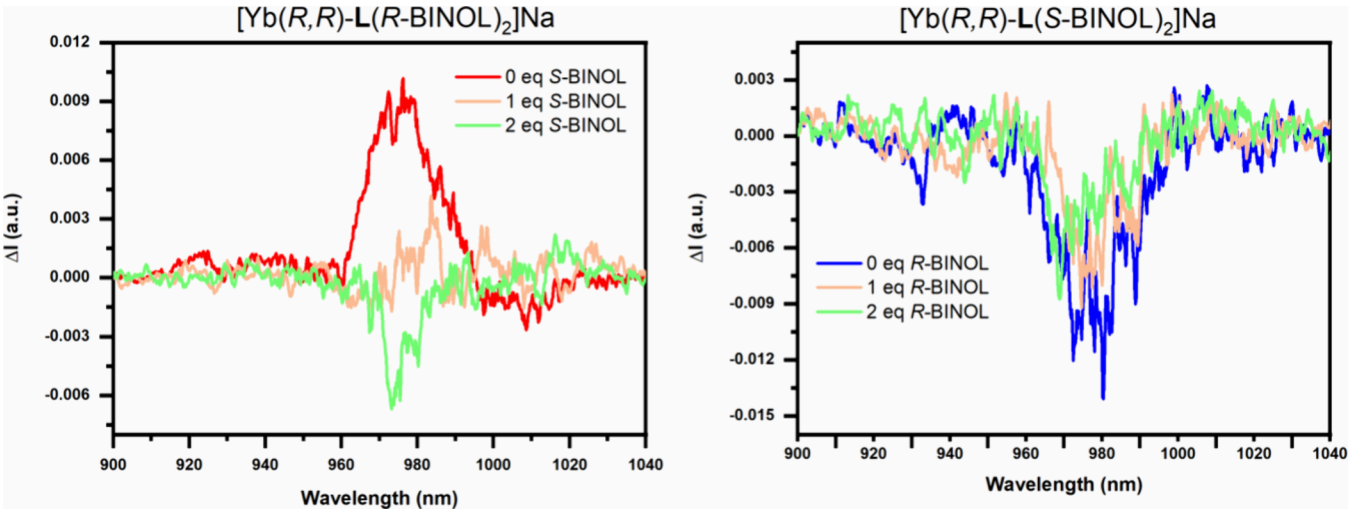

Figure 6. Changes of the CPL signature upon titration of [Yb(*R*,*R*)-**L**(*R*-BINOL)$_2$]Na with *S*-BINOL (left) and of [Yb(*R*,*R*)-**L**(*S*-BINOL)$_2$]Na with *R*-BINOL (right).

https://doi.org/10.1021/acs.inorgchem.4c05420
Inorg. Chem. 2025, 64, 5505−5512

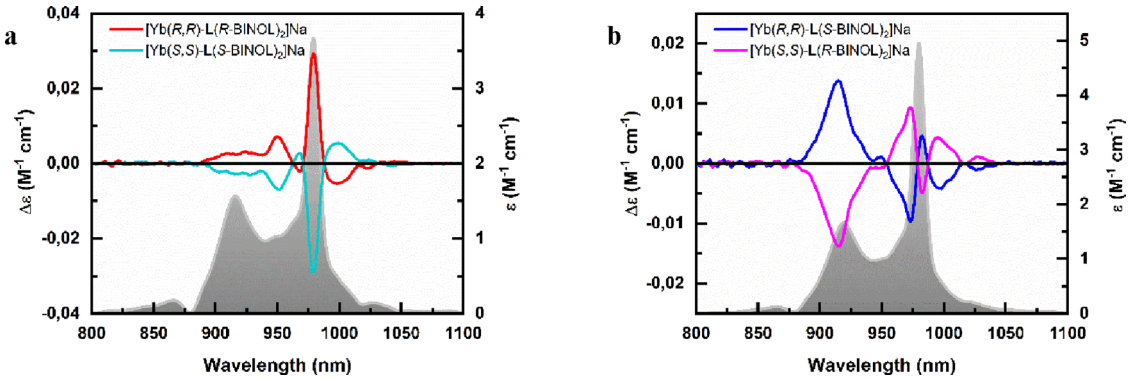

Figure 7. NIR-CD spectra of 10 mM CD_3OD solutions of the two enantiomeric couples of the investigated Yb(III) complexes. (a) [Yb(*R*,*R*)-**L**(*R*-BINOL)$_2$]Na (red)/[Yb(*S*,*S*)-**L**(*S*-BINOL)$_2$]Na (cyano) and (b) [Yb(*R*,*R*)-**L**(*S*-BINOL)$_2$]Na (blue)/[Yb(*S*,*S*)-**L**(*R*-BINOL)$_2$]Na (magenta). The molar absorption coefficient as a function of the wavelength for each couple is traced in the background.

Moreover, it is interesting to note that NIR-CD data support what was deduced through DFT calculations about the instability of heterochiral [Yb(*R*,*R*)-**L**(*R*-BINOL)(*S*-BINOL)]$^-$. More in detail, the NIR-CD signal of a 1:1:1:1 (molar ratio) solution containing Yb^{3+}, (*R*,*R*)-**L**, (*R*-BINOL), and (*S*-BINOL) is superimposable to the sum of the NIR-CD signals of the two homochiral complexes (Figure S11), confirming that the existence of the heterochiral species can be neglected. We note that the relatively large bands observed in CPL are the result of a complex overlap of transitions, possibly stemming from different M_J levels above the 0' of the excited $^2F_{5/2}$ state, which may be populated at room temperature.[52]

CONCLUSIONS

In conclusion, the synthesized C_2-symmetric [Yb**L**(BINOL)$_2$]Na complexes, characterized by the same stereochemistry of the two BINOL ligands (*S* or *R*), combine two kinds of chiralities (central and axial) in the same molecule. These stereogenic elements affect the chiroptical properties, such as CPL and CD of the Yb(III) ion: the Yb(III) CPL signal around 980 nm is mainly dictated by the BINOL stereochemistry (S → −; R → +), and the Yb(III) CD signal in the same spectral region is affected by the stereochemistry of both ligands over the entire region of the $^2F_{7/2} \rightarrow {}^2F_{5/2}$ transition. Additionally, CPL and ^{1}H NMR techniques prove the lability of BINOLate ligands in these kinds of complexes. These very interesting features can be conveniently exploited to design an optical material with easily tunable chiroptical activity, in the so important (for biological and technological applications) NIR window. In fact, dramatic changes in CD and CPL spectra around 1 μm can be obtained by simply playing with the handedness of the two chiral ligands.

ASSOCIATED CONTENT

Supporting Information

The Supporting Information is available free of charge at https://pubs.acs.org/doi/10.1021/acs.inorgchem.4c05420.

Characterization of the synthesized complexes: FT-IR of [Yb(*S*,*S*)-**L**(*R*-BINOL)$_2$]Na (Figure S1), ESI-MS of [Yb(*R*,*R*)-**L**(*R*-BINOL)$_2$]Na, [Yb(*R*,*R*)-**L**(*S*-BINOL)$_2$]Na and the related enantiomers (Figure S2). ESI-MS of [Y(*R*,*R*)-**L**(*S*-BINOL)$_2$]Na (Figure S3); ^{1}H NMR (also VT), gCOSY spectrum ^{1}H-{^{1}H} NMR spectra of [Y(*R*,*R*)-**L**(*S*-BINOL)$_2$]Na (Figures S4−S6); DFT calculation and thermodynamic study: minimum energy structures of [Lu(*R*,*R*)-**L**(*R*-BINOL)$_2$]$^-$, [Lu(*R*,*R*)-**L**(*S*-BINOL)$_2$]$^-$, and [Lu(*R*,*R*)-**L**(*R*-BINOL)(*S*-BINOL)]$^-$ (Figures S7 and S8); spectrophotometric titrations of *S*-BINOL with [Yb(*R*,*R*)-**L**](NO$_3$)$_3$ and *R*-BINOL with [Yb(*R*,*R*)-**L**](NO$_3$)$_3$ (Figure S9); chiroptical spectroscopy: ECD spectra of Yb(*R*,*R*)-**L**(*R*-BINOL)$_2$]Na and [Yb(*R*,*R*)-**L**(*S*-BINOL)$_2$]Na and related enantiomers (Figure S10); experimental and simulated NIR CD spectra of Yb^{3+} complexes (Figure S11) (PDF)

AUTHOR INFORMATION

Corresponding Authors

Silvia Ruggieri − *Luminescent Materials Laboratory, DB, University of Verona, and INSTM, UdR Verona, Verona 37134, Italy*; orcid.org/0000-0002-2849-0449; Email: silvia.ruggieri@univr.it

Fabio Piccinelli − *Luminescent Materials Laboratory, DB, University of Verona, and INSTM, UdR Verona, Verona 37134, Italy*; orcid.org/0000-0003-0349-1960; Email: fabio.piccinelli@univr.it

Authors

Oliver George Willis − *Department of Chemistry and Industrial Chemistry, University of Pisa, Pisa 56124, Italy*

Silvia Mizzoni − *Luminescent Materials Laboratory, DB, University of Verona, and INSTM, UdR Verona, Verona 37134, Italy*

Enrico Cavalli − *Department of Chemistry, Life Sciences and Environmental Sustainability, Parma University, Parma 43124, Italy*

Martina Sanadar − *Chemical Technologies Laboratory, DPIA, University of Udine, Udine 33100, Italy*

Andrea Melchior − *Chemical Technologies Laboratory, DPIA, University of Udine, Udine 33100, Italy*; orcid.org/0000-0002-5265-1396

Francesco Zinna − *Department of Chemistry and Industrial Chemistry, University of Pisa, Pisa 56124, Italy*; orcid.org/0000-0002-6331-6219

Lorenzo Di Bari − *Department of Chemistry and Industrial Chemistry, University of Pisa, Pisa 56124, Italy*; orcid.org/0000-0003-2347-2150

Giorgiana Denisa Bisag − *Department of Industrial Chemistry, University of Bologna, Bologna 40129, Italy*

https://doi.org/10.1021/acs.inorgchem.4c05420
Inorg. Chem. 2025, 64, 5505−5512

Mariafrancesca Fochi − *Department of Industrial Chemistry, University of Bologna, Bologna 40129, Italy;* orcid.org/0000-0001-9124-3304

Luca Bernardi − *Department of Industrial Chemistry, University of Bologna, Bologna 40129, Italy;* orcid.org/0000-0002-7840-3200

Complete contact information is available at: https://pubs.acs.org/10.1021/acs.inorgchem.4c05420

Notes

The authors declare no competing financial interest.

■ ACKNOWLEDGMENTS

This work was supported by the Italian Ministry for University and Research (MUR, PRIN 2017, 20172M3K5N project). The authors thank Luca Zuppiroli for the ESI-MS characterization and Emanuele Bruno Savini for performing NMR measurements, from University of Bologna. The authors from the University of Verona thank the Facility "Centro Piattaforme Tecnologiche" (CPT), for access to the Fluorolog 3 (Horiba-Jobin Yvon) spectrofluorometer. The authors from the University of Parma benefited from the equipment and support of the COMP-HUB Initiative, funded by the "Departments of Excellence" program of the Italian Ministry for Education, University and Research (MIUR, 2018-2022).

■ REFERENCES

(1) Zhang, K. Y.; Yu, Q.; Wei, H.; Liu, S.; Zhao, Q.; Huang, W. Long-Lived Emissive Probes for Time-Resolved Photoluminescence Bioimaging and Biosensing. *Chem. Rev.* **2018**, *118*, 1770−1839.

(2) Bünzli, J.-C. G. Lanthanide luminescence for biomedical analyses and imaging. *Chem. Rev.* **2010**, *110*, 2729−2755.

(3) Stachelek, P.; MacKenzie, L.; Parker, D.; Pal, R. Circularly polarised luminescence laser scanning confocal microscopy to study live cell chiral molecular interactions. *Nat. Commun.* **2022**, *13*, 553.

(4) Parker, D.; Fradgley, J. D.; Wong, K.-L. The design of responsive luminescent lanthanide probes and sensors. *Chem. Soc. Rev.* **2021**, *50*, 8193−8213.

(5) Ning, Y.; Zhu, M.; Zhang, J.-L. Near-infrared (NIR) lanthanide molecular probes for bioimaging and biosensing. *Coord. Chem. Rev.* **2019**, *399*, No. 213028.

(6) Amoroso, A. J.; Pope, S. J. A. Using lanthanide ions in molecular bioimaging. *Chem. Soc. Rev.* **2015**, *44*, 4723−4742.

(7) Bonnet, C. S.; Buron, F.; Caillé, F.; Shade, C. M.; Drahoš, B.; Pellegatti, L.; Zhang, J.; Villette, S.; Helm, L.; Pichon, C.; Suzenet, F.; Petoud, S.; Tóth, É. Pyridine-based lanthanide complexes combining MRI and NIR luminescence activities. *Chem. − Eur. J.* **2012**, *18*, 1419−1431.

(8) Piccinelli, F.; Mizzoni, S.; Zanella, G.; Gaglio, S. C.; Perduca, M.; Romeo, A.; Ruggieri, S.; Nardon, C.; Cavalli, E. Ln(III) Complexes Embedded in Biocompatible PLGA Nanoparticles as Potential Vis-to-NIR Optical Probes. *Molecules* **2023**, *28*, 2251.

(9) Cavalli, E.; Ruggieri, S.; Mizzoni, S.; Nardon, C.; Bettinelli, M.; Piccinelli, F. NIR-emission from Yb(III)- and Nd(III)-based complexes in the solid state sensitized by a ligand system absorbing in a broad UV and visible spectral window. *Results in Chemistry* **2022**, *4*, No. 100388.

(10) Cieslikiewicz-Bouet, M.; Eliseeva, S. V.; Aucagne, V.; Delmas, A. F.; Gillaizeau, I.; Petoud, S. Near-infrared emitting lanthanide(iii) complexes as prototypes of optical imaging agents with peptide targeting ability: a methodological approach. *RSC Adv.* **2019**, *9*, 1747−1751.

(11) Pan, M.; Du, B.-B.; Zhu, Y.-X.; Yue, M.-Q.; Wei, Z.-W.; Su, C.-Y. Highly Efficient Visible-to-NIR Luminescence of Lanthanide(III) Complexes with Zwitterionic Ligands Bearing Charge-Transfer Character: Beyond Triplet Sensitization. *Chem. − Eur. J.* **2016**, *22*, 2440−2451.

(12) Artizzu, F.; Mercuri, M. L.; Serpe, A.; Deplano, P. NIR-emissive erbium−quinolinolate complexes. *Coord. Chem. Rev.* **2011**, *255*, 2514−2529.

(13) Moore, E. G.; Szigethy, G.; Xu, J.; Pålsson, L.-O.; Beeby, A.; Raymond, K. N. 3,2-HOPO Complexes of Near Infra-Red (NIR) Emitting Lanthanides: Sensitization of Ho^{III} and Pr^{III} in Aqueous Solution. *Angew. Chem., Int. Ed.* **2008**, *47*, 9500−9503.

(14) Pansare, V. J.; Hejazi, S.; Faenza, W. J.; Prud'homme, R. K. Review of Long-Wavelength Optical and NIR Imaging Materials: Contrast Agents, Fluorophores, and Multifunctional Nano Carriers. *Chem. Mater.* **2012**, *24*, 812−827.

(15) Yuasa, J.; Ohno, T.; Tsumatori, H.; Shiba, R.; Kamikubo, H.; Kataoka, M.; Hasegawa, Y.; Kawai, T. Fingerprint signatures of lanthanide circularly polarized luminescence from proteins covalently labeled with a β-diketonate europium(iii) chelate. *Chem. Commun.* **2013**, *49*, 4604−4606.

(16) Orsini, S.; Zinna, F.; Biver, T.; Di Bari, L.; Bonaduce, I. Circularly polarized luminescence reveals interaction between commercial stains and protein matrices used in paintings. *RSC Adv.* **2016**, *6*, 96176−96181.

(17) Leonzio, M.; Melchior, A.; Faura, G.; Tolazzi, M.; Bettinelli, M.; Zinna, F.; Arrico, L.; Di Bari, L.; Piccinelli, F. A chiral lactate reporter based on total and circularly polarized Tb(iii) luminescence. *New J. Chem.* **2018**, *42*, 7931−7939.

(18) Willis, O. G.; Pucci, A.; Cavalli, E.; Zinna, F.; Di Bari, L. Intense 1400−1600 nm circularly polarised luminescence from homo- and heteroleptic chiral erbium complexes. *J. Mater. Chem. C* **2023**, *11*, 5290−5296.

(19) Mizzoni, S.; Sickinger, A.; Ruggieri, S.; Riobé, F.; Guy, L.; Maury, O.; Baguenard, B.; Bensalah-Ledoux, A.; Guyot, Y.; Guy, S.; Sanadar, M.; Melchior, A.; Piccinelli, F. Circularly polarized luminescence activity in the near infrared spectral region of a water-soluble ytterbium(iii) complex containing a conjugated chromophoric ligand. *New J. Chem.* **2024**, *48*, 9627−9636.

(20) Zinna, F.; Arrico, L.; Di Bari, L. Near-infrared circularly polarized luminescence from chiral Yb(iii)-diketonates. *Chem. Commun.* **2019**, *55*, 6607−6609.

(21) Ahmed, Z.; Iftikhar, K. Efficient photoluminescent complexes of 400−1800 nm wavelength emitting lanthanides containing organic sensitizers for optoelectronic devices. *RSC Adv.* **2014**, *4*, 63696−63711.

(22) Wei, H.; Yu, G.; Zhao, Z.; Liu, Z.; Bian, Z.; Huang, C. Constructing lanthanide [Nd(iii), Er(iii) and Yb(iii)] complexes using a tridentate N,N,O-ligand for near-infrared organic light-emitting diodes. *Dalton Trans.* **2013**, *42*, 8951−8960.

(23) Katkova, M. A.; Pushkarev, A. P.; Balashova, T. V.; Konev, A. N.; Fukin, G. K.; Ketkov, S. Y.; Bochkarev, M. N. Near-infrared electroluminescent lanthanide [Pr(iii), Nd(iii), Ho(iii), Er(iii), Tm(iii), and Yb(iii)] N,O-chelated complexes for organic light-emitting devices. *J. Mater. Chem.* **2011**, *21*, 16611−16620.

(24) Bradley, J. D. B.; Pollnau, M. Erbium-doped integrated waveguide amplifiers and lasers. *Laser Photonics Rev.* **2011**, *5*, 368−403.

(25) Richardson, F. S. Selection rules for lanthanide optical activity. *Inorg. Chem.* **1980**, *19*, 2806−2812.

(26) Moore, E. G.; Samuel, A. P.; Raymond, K. N. From antenna to assay: lessons learned in lanthanide luminescence. *Acc. Chem. Res.* **2009**, *42*, 542−552.

(27) Leif, R. C.; Vallarino, L. M.; Becker, M. C.; Yang, S. Increasing the luminescence of lanthanide complexes. *Cytometry, Part A* **2006**, *69A*, 767−778.

(28) De Sà, G. F.; Malta, O. L.; de Mello Donegá, C.; Simas, A. M.; Longo, R. L.; Santa-Cruz, P. A.; da Silva, E. F., Jr Spectroscopic properties and design of highly luminescent lanthanide coordination complexes. *Coord. Chem. Rev.* **2000**, *196*, 165−195.

(29) Doffek, C.; Alzakhem, N.; Bischof, C.; Wahsner, J.; Guden Silber, T.; Lugger, J.; Platas-Iglesias, C.; Seitz, M. Understanding the

Quenching Effects of Aromatic C−H- and C−D-Oscillators in Near-IR Lanthanoid Luminescence. *J. Am. Chem. Soc.* **2012**, *134*, 16413−16423.
(30) Zhang, J.-X.; Chan, W.-L.; Xie, C.; Zhou, Y.; Chau, H.-F.; Maity, P.; Harrison, G. T.; Amassian, A.; Mohammed, O. F.; Tanner, P. A.; Wong, W.-K.; Wong, K.-L. Impressive near-infrared brightness and singlet oxygen generation from strategic lanthanide−porphyrin double-decker complexes in aqueous solution. *Light: Sci. Appl.* **2019**, *8*, 46.
(31) Brito-Santos, G.; Gil-Hernández, B.; Martín, I. R.; Guerrero-Lemus, R.; Sanchiz, J. Visible and NIR emitting Yb(iii) and Er(iii) complexes sensitized by β-diketonates and phenanthroline derivatives. *RSC Adv.* **2020**, *10*, 27815−27823.
(32) Cavalli, E.; Nardon, C.; Willis, O. G.; Zinna, F.; Di Bari, L.; Mizzoni, S.; Ruggieri, S.; Gaglio, S. C.; Perduca, M.; Zaccone, C.; Romeo, A.; Piccinelli, F. Near Infrared Circularly Polarized Luminescence From Water Stable Organic Nanoparticles Containing a Chiral Yb(III) Complex. *Chem. − Eur. J.* **2022**, *28*, No. e202200574.
(33) Arrico, L.; Di Bari, L.; Zinna, F. Quantifying the Overall Efficiency of Circularly Polarized Emitters. *Chem. - A Eur. J.* **2021**, *27*, 2920−2934.
(34) Mukthar, N. F. M.; Schley, N. D.; Ung, G. Strong Circularly Polarized Luminescence at 1550 nm from Enantiopure Molecular Erbium Complexes. *J. Am. Chem. Soc.* **2022**, *144*, 6148−6153.
(35) Deng, M.; Schley, N. D.; Ung, G. High circularly polarized luminescence brightness from analogues of Shibasaki's lanthanide complexes. *Chem. Commun.* **2020**, *56*, 14813−14816.
(36) Sasai, H.; Suzuki, T.; Itoh, N.; Tanaka, K.; Date, T.; Okamura, K.; Shibasaki, M. Catalytic asymmetric nitroaldol reaction using optically active rare earth BINOL complexes: investigation of the catalyst structure. *J. Am. Chem. Soc.* **1993**, *115*, 10372−10373.
(37) Brunel, J. M. BINOL: A Versatile Chiral Reagent. *Chem. Rev.* **2005**, *105*, 857−898.
(38) Mukthar, N. F. M.; Schley, N. D.; Ung, G. Strong Circularly Polarized Luminescence at 1550 nm from Enantiopure Molecular Erbium Complexes. *J. Am. Chem. Soc.* **2022**, *144*, 6148−6153.
(39) Frisch, M. J.; Trucks, G. W.; Schlegel, H. B.; Scuseria, G. E.; Robb, M. A.; Cheeseman, J. R.; Scalmani, G.; Barone, V.; Petersson, G. A.; Nakatsuji, H.; Li, X.; Caricato, M.; Marenich, A. V.; Bloino, J.; Janesko, B. G.; Gomperts, R.; Mennucci, B.; Hratchian, H. P.; Ortiz, J. V.; Izmaylov, A. F.; Sonnenberg, J. L.; Williams-Young, D.; Ding, F.; Lipparini, F.; Egidi, F.; Goings, J.; Peng, B.; Petrone, A.; Henderson, T.; Ranasinghe, D.; Zakrzewski, V. G.; Gao, J.; Rega, N.; Zheng, G.; Liang, W.; Hada, M.; Ehara, M.; Toyota, K.; Fukuda, R.; Hasegawa, J.; Ishida, M.; Nakajima, T.; Honda, Y.; Kitao, O.; Nakai, H.; Vreven, T.; Throssell, K.; Montgomery, J. A.; Peralta, J. E.; Ogliaro, F.; Bearpark, M. J.; Heyd, J. J.; Brothers, E. N.; Kudin, K. N.; Staroverov, V. N.; Keith, T. A.; Kobayashi, R.; Normand, J.; Raghavachari, K.; Rendell, A. P.; Burant, J. C.; Iyengar, S. S.; Tomasi, J.; Cossi, M.; Millam, J. M.; Klene, M.; Adamo, C.; Cammi, R.; Ochterski, J. W.; Martin, R. L.; Morokuma, K.; Farkas, O.; Foresman, J. B.; Fox, D. J. *Gaussian 16* Rev.A03 Gaussian Inc.: Wallingford, CT, 2016.
(40) Da Chai, J.; Head-Gordon, M. Long-range corrected hybrid density functionals with damped atom−atom dispersion corrections. *Phys. Chem. Chem. Phys.* **2008**, *10*, 6615−6620.
(41) Cao, X.; Dolg, M. *J. Mol. Struct. THEOCHEM* **2002**, *581*, 139.
(42) Tomasi, J.; Mennucci, B.; Cammi, R. Quantum Mechanical Continuum Solvation Models. *Chem. Rev.* **2005**, *105*, 2999−3094.
(43) Piccinelli, F.; Speghini, A.; Monari, M.; Bettinelli, M. New chiral pyridine-based Eu(III) complexes: Study of the relationship between the nature of the ligands and the $^5D_0$ luminescence spectra. *Inorg. Chim. Acta* **2012**, *385*, 65−72.
(44) Di Bari, L.; Lelli, M.; Pintacuda, G.; Pescitelli, G.; Marchetti, F.; Salvadori, P. Solution versus Solid-State Structure of Ytterbium Heterobimetallic Catalysts. *J. Am. Chem. Soc.* **2003**, *125*, 5549−5558.
(45) Di Bari, L.; Lelli, M.; Salvadori, P. Ligand Lability and Chirality Inversion in Yb Heterobimetallic Catalysts. *Chem. − Eur. J.* **2004**, *10*, 4594−4598.
(46) Bui, A. T.; Beyler, M.; Grichine, A.; Duperray, A.; Mulatier, J.-C.; Guyot, Y.; Andraud, C. l.; Tripier, R.; Brasselet, S.; Maury, O. Near infrared two photon imaging using a bright cationic Yb(III) bioprobe spontaneously internalized into live cells. *Chem. Commun.* **2017**, *53*, 6005−6008.
(47) Zhang, T.; Zhu, X.; Cheng, C. C. W.; Kwok, W.-M.; Tam, H.-L.; Hao, J.; Kwong, D. W. J.; Wong, W.-K.; Wong, K.-L. Water-Soluble Mitochondria-Specific Ytterbium Complex with Impressive NIR Emission. *J. Am. Chem. Soc.* **2011**, *133*, 20120−20122.
(48) Nonat, A.; Imbert, D.; Pécaut, J.; Giraud, M.; Mazzanti, M. Structural and photophysical studies of highly stable lanthanide complexes of tripodal 8-hydroxyquinolinate ligands based on 1,4,7-triazacyclononane. *Inorg. Chem.* **2009**, *48*, 4207−4218.
(49) Gupta, S. K.; Kadam, R. M.; Pujari, P. K. Lanthanide spectroscopy in probing structure-property correlation in multi-site photoluminescent phosphors. *Coord. Chem. Rev.* **2020**, *420*, No. 213405.
(50) Kreidt, E.; Kruck, C.; Seitz, M. *Handbook on the physics and chemistry of rare earths*; Elsevier, 2018, *53*, 35.
(51) Weber, M. J. Radiative and Multiphonon Relaxation of Rare-Earth Ions in Y_2O_3. *Phys. Rev.* **1968**, *171*, 283−291.
(52) Sickinger, A.; Grasser, M.; Baguenard, B.; Bensalah-Ledoux, A.; Guy, L.; Bui, A. T.; Guyot, Y.; Dorcet, V.; Pointillart, F.; Cador, O.; Guy, S.; Maury, O.; Le Guennic, B.; Riobé, F. Temperature-dependent NIR-CPL spectra of chiral Yb(III) complexes. *Phys. Chem. Chem. Phys.* **2024**, *26*, 15776−15783.

https://doi.org/10.1021/acs.inorgchem.4c05420
Inorg. Chem. 2025, 64, 5505−5512